24th COBEM - 2017

24th ABCM International Congress of Mechanical Engineering
December 3-8, 2017, Curitiba, PR, Brazil

COBEM-2017-0706
EFFECT OF AIR-FUEL RATIO ON SYNGAS COMBUSTION IN AN OPTICALLY ACCESSIBLE SPARK IGNITION ENGINE

Santiago Daniel Martinez Boggio
Pedro Texeira Lacava
Maycon Ferreira Silva
Technological Institute of Aeronautics, Laboratory of Combustion, Propulsion and Energy, São José dos Campos, SP, Brazil
santiagofing@gmail.com

Simona Merola
Adrian Irimescu
Istituto Motori, CNR, Napoli, Italy
s.merola@im.cnr.it

Pedro Luis Curto Risso
University of La República, Department of Applied Thermodynamics, Montevideo, Uruguay
pcurto@fing.edu.uy

Abstract. *Biomass gasification converts a solid fuel into a gaseous mixture (Syngas) which can be burnt in reciprocating internal combustion engines (ICE). The introduction of new policies, aimed at reducing the green-house gases emissions and the dependence of fossil fuels, promotes the use of alternative fuels in both transportation and power generation. To this aim, the paper presents an experimental investigations performed to study the effect of air-fuel ratio on the combustion process in a port fuel injection spark-ignition engine fueled with an equivalent Syngas mixture. Methane was considered as baseline fuel. The in-cylinder pressure and the related parameters were analyzed as indicators of the combustion behavior. 2-D digital cycle resolved imaging measurements were performed to evaluate the flame propagation. The engine was operated at fixed rotational speed (900 rev/min) at wide open throttle. The excess air ratio was raised from 1.0 to 1.4 (close to the flammability limit of methane) and spark timing was adopted according to the maximum brake torque of the baseline fuel to compare the different cases in the same fluid dynamic conditions at ignition. Cycle-to-cycle variability was below 4% for both fuels and air fuel ratios tested, indicating a stable combustion process. However Syngas mixtures allowed more stable engine operation at the lean burn limit than Methane showing a significant decrease in the coefficient of variation measured for the IMEP. Finally, a decrease of the combustion duration for Syngas was observed as consequence of hydrogen content.*

Keywords: *Combustion, SI Engine, Syngas, Methane, Flame visualization.*

1. INTRODUCTION

Despite high growth rates, renewable energy still represents only a small fraction of today's global energy consumption. Renewable electricity generation (excluding hydroelectric), is estimated to account for nearly 8% of global electricity generation. Renewables do, however, play a significant role in the growth of electricity, contributing almost 40% of the growth in global power generation in 2016 (EIA, 2017). In volume terms, the largest increase was in China, followed by the US; with Japan, India and Brazil making up the rest of the top five (Avinash, 2017). Specially, in Brazil the thermoelectric generation represents the 28% of power generation in 2016 below the hydroelectric generation. Moreover, Biomass represents the 37% of the fuel matrix used for thermoelectric generation just behind natural gas (EPE, 2017). Therefore, Biomass has a considerable potential as fuel for electric power generation as complementary or as a future substitute for Natural Gas.

Gaseous fuels have become a good alternative to traditional petroleum derived fuels, such as diesel and gasoline. Hence, compressed natural gas (CNG) has been successfully used for many years as fuel in engines, mainly due to its abundance in nature and its low expensive extraction (Catapano et al., 2013). Natural gas surpassed coal in 2017 as the most common source for electricity generation in the United States (EIA, 2017). The main component (80-90%) of compressed natural gas is methane (CH_4). It is characterized by a high octane number and increased auto-ignition

temperature, which make it an effective fuel substitute for gasoline in spark ignition (SI) engines (Catapano et al., 2013). It represents an immediate advantage over other hydrocarbon fuels because of the lower C/H ratio resulting in reduced CO_2 emissions (Di Iorio, 2014).

Syngas has also received great interest as fuel for engines, especially in applications involving combined power and heat generation (Arroyo et al., 2015). This gas is composed of hydrogen (H_2), carbon monoxide (CO), diluents and smaller percentage of methane (CH_4) among others (Arroyo et al., 2015). The final composition may vary depending on the process of production, the raw material as well as the subsequent gas treatment. Therefore, such gas mixtures are characterized by high variability in composition. The main drawback of Syngas is its lower calorific value compared with natural gas, caused by the high fraction of inert gases in its composition, which causes that part of the energy released in combustion was absorbed by these components instead of generating power (Bika et al., 2011). Also, the presence of inert gases displaces air in the intake manifold when PFI mode of injection is used, thus the volumetric efficiency decreases, resulting in lower the power output (Bika et al., 2011). Flame stability is another problem encountered in the combustion of syngas fuels, given their low calorific values (Shivapuji et al., 2015). In order to avoid the effects of its low calorific value, syngas can be upgraded by removing fractions of inert gases, obtaining gaseous fuels with a composition closer to than of natural gas, but with renewable origin (Shivapuji et al., 2015). Together with these upgrading methods, the recent development of new catalysts has opened a wide field oriented toward the production of improved gaseous fuels with great performance for engines (Hagos et al., 2014). Therefore, compressed natural gas (CNG/CH_4) and synthesis gas (Syngas) have considerable potential as alternative fuels for internal combustion engines (Martinez et al., 2012).

Starting from these considerations, deeper understanding of thermal and fluid-dynamic phenomena that occur in the combustion chamber of engines due to the use of alternative gaseous fuels is necessary, especially to adopt syngas as replacement for fossil-derived fuels. To this goal, the present work shows the results obtained by experimental activities carried out on an optically accessible single cylinder PFI SI engine fueled with methane and equivalent syngas. This study was performed at fixed low speed and maximum load, representative of stationary applications. The analysis of the combustion process was done through combined thermodynamic and optical investigations. In particular, digital cycle resolved imaging was obtained with high spatial resolution in the combustion chamber to characterize the flame propagation in terms of size, velocity, center displacement and circularity.

2. EXPERIMENTAL PROCEDURE

All tests were performed on an optically accessible single cylinder PFI-SI engine AVL 5406 (Fig. 1a). The head had four valves and a spark plug located 5mm from the center of the combustion chamber (Fig. 1b). Optical accessibility was provided via an elongated piston with a wide flat sapphire window in the head and a quartz ring replacing the upper part of the cylinder liner. To reduce window contamination by lubricating oil, self-lubricating Teflon-bronze piston rings were used in the optical section. During combustion, the light emission passed through the sapphire window and was reflected toward the optical detection assembly by a 45° inclined UV-visible mirror located in the elongated piston, and then recorded by the acquisition system aimed at studying flame front propagation. The optical set-up allowed a bottom field of view that corresponded to 78% of the piston diameter and 61% of piston area (Fig. 1b).

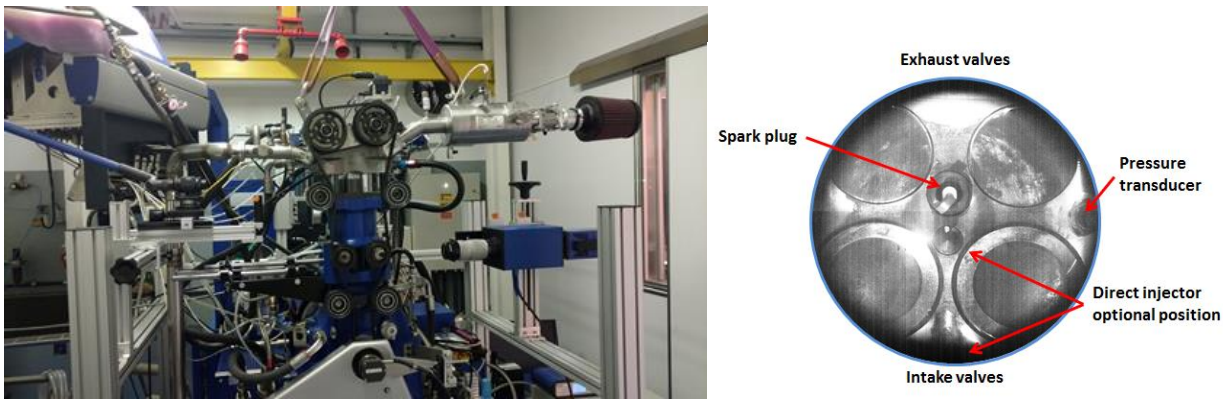

Figure 1. Experimental setup. (a) Single cylinder research engine and the optical experimental arrangement; (b) cylinder head bottom view from inclined mirror located below the piston.

The crankshaft was equipped with a shaft encoder resolving 1800 increments per revolution. An AVL427 engine-timing unit was employed for ignition and injection control, as well as for provision of synchronized triggering for image acquisition and in- cylinder pressure recording. Further details of engine specification are shown in Table 1.

The fuels used for these experiments were a syngas equivalent mixture (17.1% H_2, 34.3% CO, 8.6% CH_4, 20% CO_2 and 20% N_2) and methane, used as baseline fuel. The syngas mixture was selected as representative of gasification from a bubbling fluidized bed (Magalhaes, 2011). Table 2 shows the main characteristics of the investigated fuels.

Table 1. Specifications of the PFI SI single cylinder research engine.

Component	*Size*	*Unit*
Total volume	530	cm^3
Piston bore	82	mm
Stroke	90	mm
Compression ratio	9.7:1	-
Number of valves	4	2 int, 2 exh
Connecting rod	144	mm
Intake valve diameter	34	mm
Exhaust valve diameter	26	mm
Open Intake Valve	718	CAD
Close Intake Valve	204	CAD
Open Exhaust Valve	480	CAD
Close Exhaust Valve	716	CAD
Intake valve lift	10.49	mm
Exhaust valve lift	9.25	mm

Table 2. Main properties of the fuel tested.

Properties	*Methane*	*Syngas*
LHV (MJ/kg)	50.2	8.1
Stoichiometric Air fuel ratio (kg air/kg fuel)	17.2	2.3
Molecular weight (kg/kmol)	16.0	25.7
Peak flame temp (K @1 atm)	2226	2112
Laminar Flame Speed (cm/sec @1Atm, 293K, λ=1.0)	35.7	42.0
CH_4/H_2	-	0.5
CO/H_2	-	2.0
Degree of Dilution (DOD) (%)	0	40

The experiments were performed at 900 RPM engine speed and wide open throttle, as a representative point of electric power generation applications, with the engine operated at full load for extensive periods. All timings given in CAD refer to 'Crank Angle Degree', with one 1 CAD corresponding to 0.185 ms at 900 RPM speed used throughout this study. The engine was equipped with two direct injection systems optional to the port-fuel injection configuration. In this work PFI assessment was used as the most representative for SI engine with gaseous fuelling. Air-fuel ratio was set at stoichiometric value, and then was increased until the flammability limit of methane (λ=1.4) was reached. The performance and stability of the engine were evaluated through the indicated mean effective pressure (IMEP) and related Coefficient of Variation (COV_{IMEP}) (Heywood, 1988). The relative air fuel ratio was measured using a wide band exhaust gas oxygen sensor, with an accuracy of ±1%. Injection pressure was maintained at 7 bar for all conditions, as pressure of design of the injector Bosch ML082G created to operate with gaseous fuels in port fuel configuration. Coolant and lubricant temperature were maintained at 330-335 K using a thermal conditioning unit; intake air temperature was in range of 300 K and ambient pressure was around 1 bar. Spark advance (SA) was fixed at 7 CAD BTDC that corresponded to the maximum brake torque (MBT) of methane in stoichiometric condition. The same SA allowed to analyze the flame propagation and combustion behavior at same fluid dynamics conditions (Merola et al. 2016).

For each engine operative condition, tests were performed according to a procedure of 1 minute of warm-up in motored conditions, followed by firing until a stable lambda value was obtained (around 15 seconds), after which 200 consecutive cycles were recorded. In-cylinder pressure was acquired with an accuracy of ±1% by using a quartz pressure transducer flush-installed in the region between the intake valves; crank angle resolution was 0.1 CAD. Based on this data, the rate of heat release and related parameters were evaluated. Optical data were detected in the last 25 cycles of the sets of 200 in order to retrieve information from more stable combustion conditions. Pressure values, as well as the image sequences were related to piston movement by triggering the data acquisition system in gated mode. Heat release analysis was performed by a simplified approach based on the first law of thermodynamics (Heywood,

1988) and mass fraction burned (MFB) was calculated based on the integral heat release (Irimescu et al. 2014). More details on the thermodynamic analysis can be found in (Martinez et al, 2017).

2.1 Optical Measurements

Flame front propagation was investigated by cycle resolved digital imaging. A high speed 12 bit CMOS (PCO Dimax S1) camera was coupled with a double intensifier (Video Scope VS4-1845HS). The assembly allowed a high sensitivity in the spectral range from 290 nm to 700 nm, with 50% quantum efficiency at 450 nm. The camera could work in full chip configuration (1008x1008 pixel) with a maximum frame rate of 4467 fps. In order to improve the acquisition speed a region of interest of 864x896 pixel was selected; this permitted to reach a frame rate of 5400 fps, corresponding to 1 image/CAD at 900 rpm (1 CAD = 185 μs). The detection system was equipped with UV-Nikkor 105 mm f/4.5 lens. To improve the signal to noise ratio, the level of the intensification was increased by 30% at increasing λ value. Moreover, the f/stop of the objective was maintained at f/11 for methane and f/4.5 for all the tests on syngas fuels. The optical setup allowed to detect image sequences with a spatial resolution of 91 μm/pixel. For all the optical measurements, the synchronization between the cameras and the engine was achieved through the crank angle encoder signal and the unit delay.

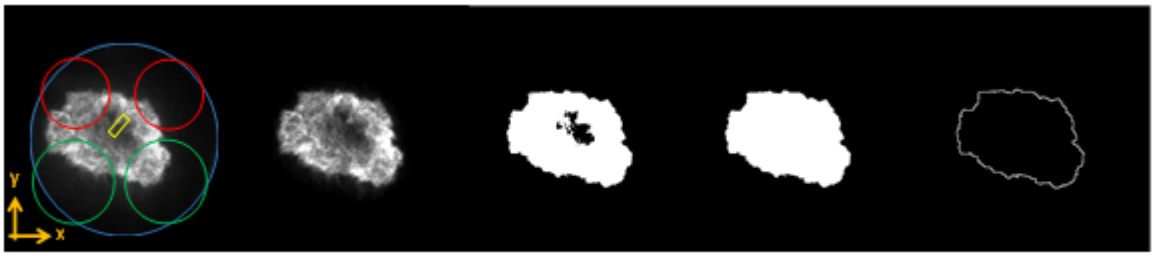

Figure 2. Sketch of the image processing steps; intake, exhaust valves and optical limit are also shown.

The application of a custom procedure of image processing allows a detailed analysis of flame morphology (Merola et al., 2017). Specifically, by using a routine developed in Vision of National Instruments (Vision Assistant 2016, NI ACADEMIC SITE LICENSE, Austin, Texas, USA), CMOS 8-bit images were treated to retrieve geometrical parameters of the flame front. Following the procedure sketched in Fig. 2, after the extraction of the intensity level, a circular mask was fixed in order to cut light from reflections at the boundaries of the optical access (Fig. 2a). Successively, the image processing adjusted the contrast and brightness of the images with respect to the maximum intensity value in order to optimize the signal to noise ratio (Fig. 2b). Then, a threshold was applied to obtain binary images, with 1 (white) associated to a pixel belonging to the object (foreground) and 0 (black) was referred to the background (Fig. 2c). In this work automatic threshold operation (metric method) based on locally adaptive algorithm was used (Parker, 2010). After this step, morphological transformations were applied to fill holes and remove small objects that were not part of the flame and could bias the evaluation of morphological parameters (Fig 2d). Finally the outline border of the flame was extracted (Fig. 2e). More details on the procedure are given in (Martinez et al, 2017). The image processing estimated the clamp distances (D_x and D_y) and the flame centroid (CDM) coordinates, both in x and y directions. Moreover, the Heywood circularity factor (HF) was evaluated. The maximum clamp of the flame front represented the distance between the furthest opposed points on the edge found in the image along the horizontal (x) and vertical (y) direction. In a perfect circle this two parameters would be equal. Therefore, their ratio intrinsically allowed the retrieval of information on flame front distortion. Moreover, the average value between D_x and D_y was considered as representative of the mean flame diameter (D_m). Flame speed was calculated as the incremental ratio between two frames of D_m with respect to the dwell time. The flame centroid (CDM) was the arithmetical center of luminosity evaluated for a binary image. It was identified by the x and y coordinates with respect to the Cartesian system fixed in the center of the combustion chamber. The Heywood circularity factor (HF) was used to follow the evolution of flame front distortion. The shape factor corresponded to the ratio between the flame front perimeter and the circumference length of a circle with the same area of the flame.

3. RESULTS AND DISCUSSION

A global analysis of the combustion process determined by the selected operative conditions, was performed by a thermodynamic approach. The evolutions of in-cylinder pressure and Mass Burn Fraction (MFB) were analyzed as average traces for 200 consecutive acquisitions; results are reported in Fig. 3. The motored pressure signal (gray line) is also shown in Fig. 3a as reference; pressure levels are slightly higher during compression with respect to fired operation, given that the working fluid contained only air. For the stoichiometric air-fuel ratio, due to the non-optimized

spark timing for syngas, methane showed higher peak pressure and slower decrease in the last combustion stage, together with better performance and stability (Table 3). Also, the high content of inert gas reduce the LHV of Syngas (Table 2), therefore the amount of fuel that is necessary to inject is greater. The increase of duration of injection (DOI, Table 3) implies a reduction of volumetric efficiency and decrease the performance of the engine. However, the mass fraction burned (MFB) curves (Fig.3b) presented a higher 'burning speed' in the early combustion stages for syngas. For lean burn case with λ=1.2 a significant evolution in the pressure signals was observed. The trace related to syngas, due to the presence of hydrogen, was closer to methane, with an evident improvement of the burning speed in the first stage of the combustion. A slight improvement in terms of performance and stability was also observed. The burn duration of syngas resulted still shorter than methane, showing a faster decrease in pressure during the expansion stroke, after the peak pressure. For the case of lambda 1.4, larger differences were found in the thermodynamic behaviour. The maximum pressure value for methane resulted quite delayed and comparable with the motored signal due to the fact that the lean flammability limit was reached; this induced a strong decrease in the initial combustion speed and in engine stability. On the contrary, only a slight decrease in performance and stability was observed for syngas fuel, despite the non-optimized spark timing setting. Additionally, a shorter flame development and propagation duration was detected for syngas with respect to methane. This behavior demonstrated the strong potentiality of syngas as an alternative gaseous fuel for SI engines. The results agree with other experiments (Di Iorio et al., 2015) in which a direct correlation was demonstrated between the shortening of the combustion process and improvement of combustion stability.

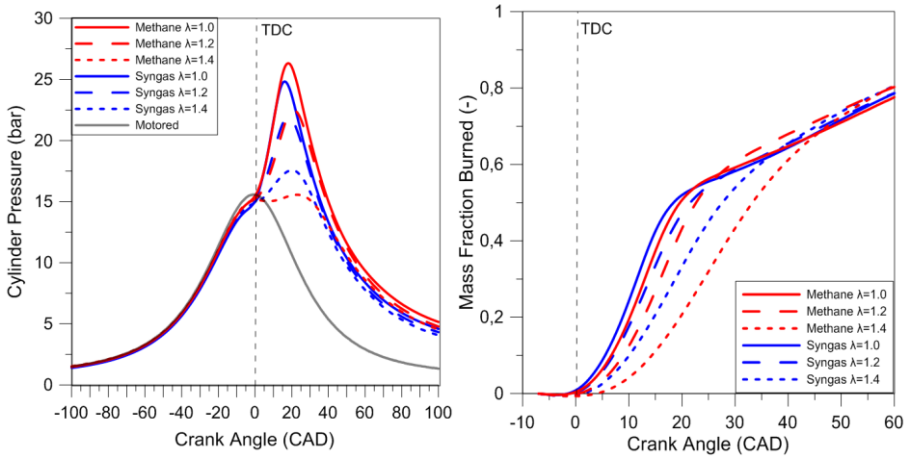

Figure 3. (a) In-cylinder pressure traces and (b) Mass burn fraction averaged over 200 consecutive cycles for the selected air-fuel ratios and fuels.

Table 3. Thermodynamics results evaluated on 200 consecutive cycles.

Fuel	*Lambda (-)*	*DOI (CAD)*	*IMEP (bar)*	*Cov IMEP (%)*	*Pmax (bar)*	*Cov Pmax (%)*	*Angle Pmax (CAD ATDC)*
Methane	1.0	61	5.4	0.6	26.7	3.3	18.1
	1.2	50	4.8	0.8	22.7	4.7	20.8
	1.4	43	3.9	3.4	15.9	5.5	22.8
Syngas	1.0	320	4.6	0.9	24.9	2.3	16.2
	1.2	265	4.2	0.5	22.0	3.1	18.3
	1.4	245	3.6	1.2	17.7	4.5	20.0

Even if the in-cylinder pressure measurements allow a comprehensive analysis of combustion characteristics, they do not furnish detailed results of the local distribution of the burned mass, flame behaviour inside the combustion chamber and on the speed of flame propagation. In this sense, cycle resolved visualization represents a powerful tool for quantitative analysis of flame front propagation. Fig. 4 shows a selection of images detected in stoichiometric and lean burn conditions (λ=1.4) for both fuels. It should be noted that each column of images was chosen at roughly the same flame area size, thus at different crank angles after start of spark (ASOS). In this way, the images correspond to 5%, 10%, 20%, 30%, 40% and 60% flame area, referenced to the cylinder cross section.

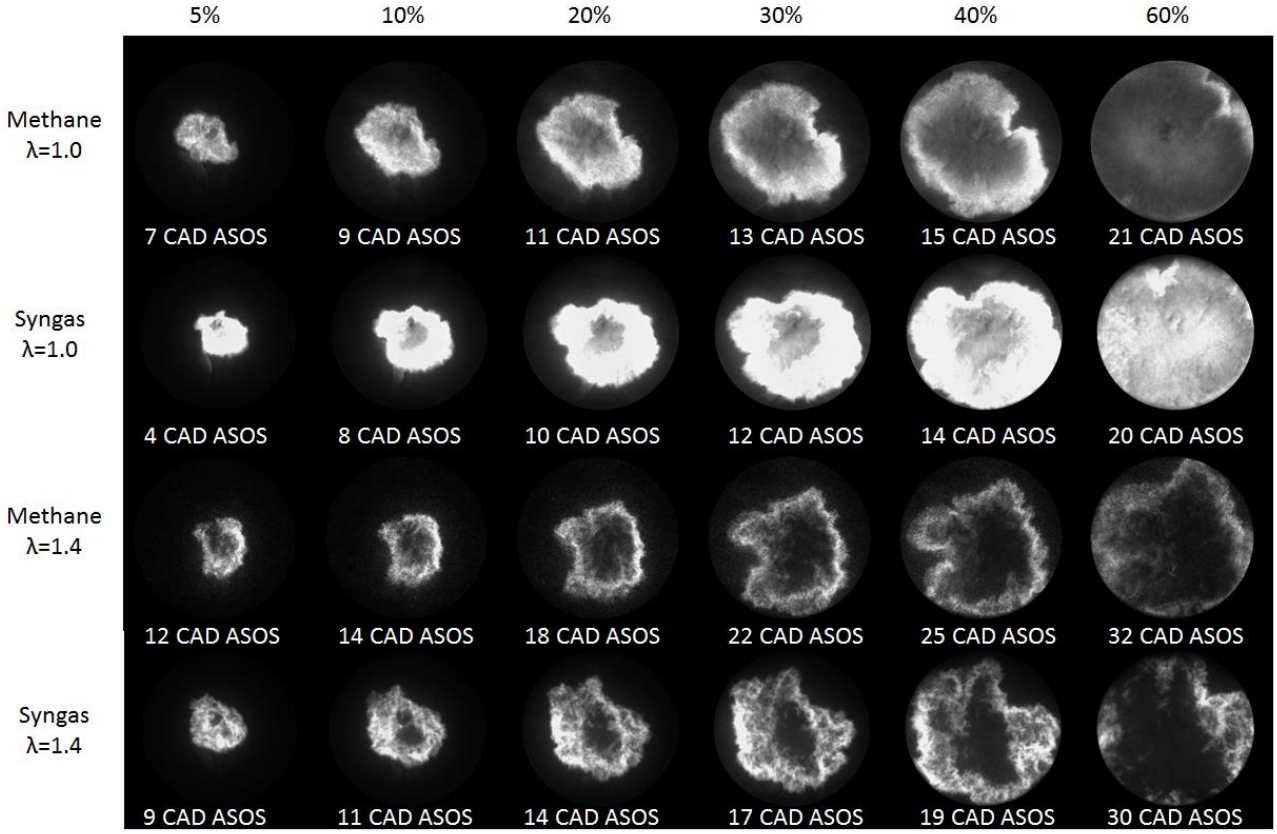

Figure 4. Flame image sequence for methane and syngas with two air fuel ratios in 5%, 10%, 20%, 30%, 40% and 60% of the piston area.

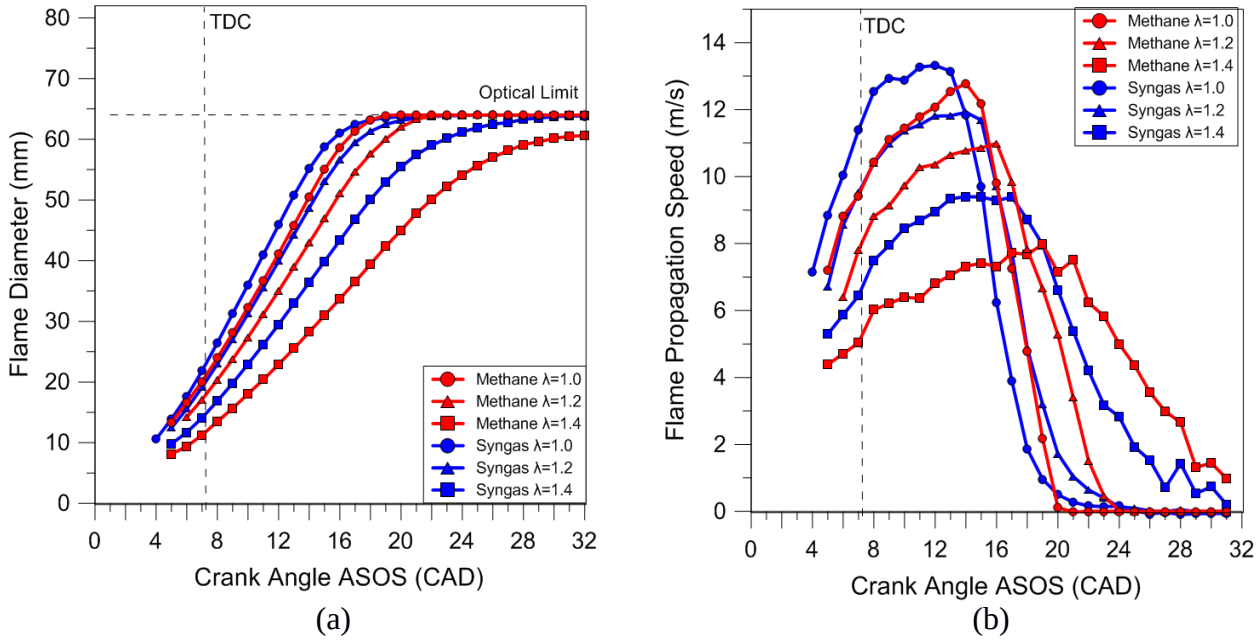

Figure 5. Evolution of the flame front a) Diameter and b) Flame speed propagation for lambda 1.0 to 1.4 both obtained by averaged data over 25 consecutive engine cycles.

By applying the image processing previously described, the trends of mean diameter and propagation speed of the flame were obtained. Results reported in Fig. 5 are related to the averaged values on 25 consecutive engine cycles. It is clear that flame diameter evolved similarly to MFB. Methane flames were slower and the gap with syngas increased at

increasing air-fuel ratio, even without adjusting the spark advance. Hence the presence of hydrogen improved the propagation of the flame more than the slowdown effect of dilution through inert gases. To better investigate the effect of fuels on the initial flame propagation, the flame diameter in correspondence of 5% MFB was calculated. It is noticeable that the position of the 5% MFB was taken from thermodynamic analyses (Fig.3b) for each fuel and air fuel ratio. Therefore, for each test condition a value of MFB position from the average trace was extracted. Results related to stoichiometric and lean burn condition for 25 consecutive optical acquisitions are shown in Fig. 6. These allowed an intrinsic evaluation of the cycle-by-cycle variability induced on the flame kernel development by the air-fuel ratio and fuel composition. The slight difference in the mean value of the flame diameter (<1% with respect to the piston cross section) was determined by a difference in the flame penetration along the piston stroke direction. In particular, at fixed MFB, higher flame penetration was observed for syngas compared to methane, and in stoichiometric conditions with respect to lean burn cases. Regarding the spread of the data, as expected, an increase in the variability of the flame diameter was observed at increasing lambda values; this was more significant for methane, demonstrating a better stability of the syngas flame propagation during the early stage of combustion. Moreover, the coefficient of variation (Cov) related to the flame diameter resulted linkable to the Cov of in-cylinder peak pressure, confirming the importance of controlling the stability of combustion, especially during the flame kernel development stage.

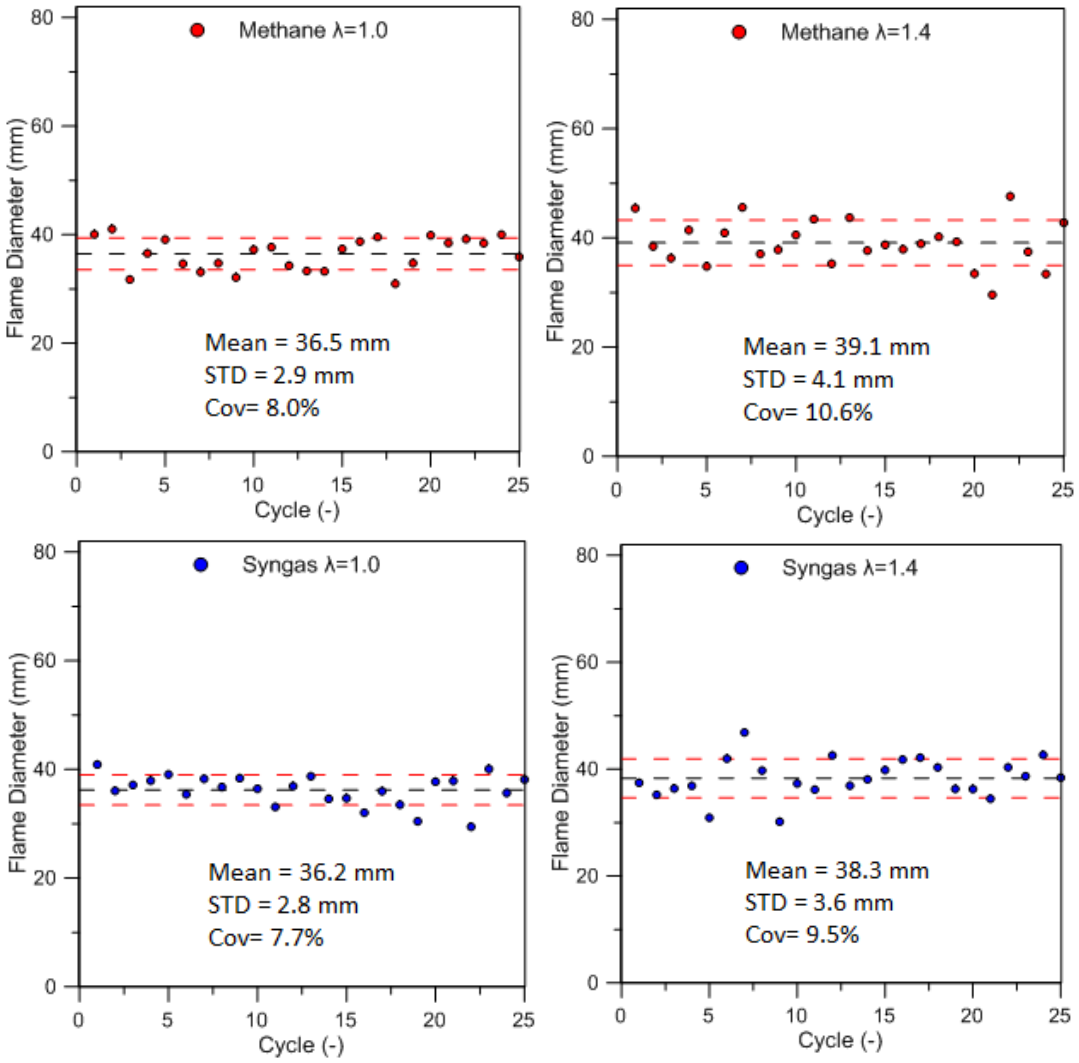

Figure 6. Flame diameter measured for 25 engine cycles in correspondence of 5% MFB for both the fuels in stoichiometric and lean burn (λ=1.4) conditions. Statistics parameters are also reported in the plots.

To better understand the effect of the fuels and air dilution on the early combustion stages, the flame front shape at 5% MFB was evaluated by analyzing the Heywood Factor. Results reported in Fig. 7 clearly demonstrated that during stoichiometric combustion the flame propagated quite uniformly in all directions, even if syngas flame fronts resulted a little more “circular” than methane. In lean burn condition, the simultaneous action of the flow field and fuel charge distribution determined a strong increase in the flame distortion of methane, while the effect was feeble for syngas. It is

interesting to observe that the the air dilution influenced the cyclic variability of the flame front shape more than the size. These results agree with those obtained by the analysis of the luminous centroid (CDM) position. Fig. 8 shows CDM values measured for 25 engine cycles in correspondence of 5% MFB for both fuels in stoichiometric and lean burn (λ=1.4) conditions; the spark plug position is also skectched. Moreover the spatially average values are indicated as "cross" symbols. As expected, for stoichiometric air fuel ratio, syngas presented a position closer to the combustion center and spark plug, compared to that for methane; moreover, the CDM values were distributed on a smaller area. This can be associated to a faster flame speed, as confirmed by the increase in flame displacement at increasing lambda value. Moreover, a preferential propagation towards the intake valves was observed, due to the effect of flow field (tumble motion) on the flame propagation for both fuels and air fuel ratios.

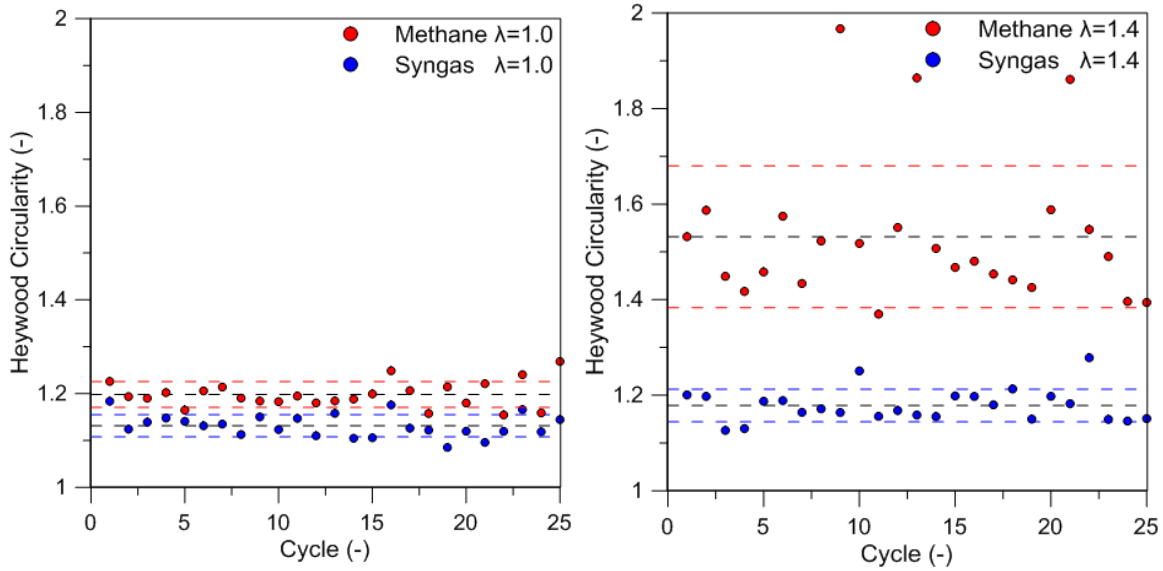

Figure 7. Heywood circularity factor measured for 25 engine cycles in correspondence of 5% MFB for both the fuels in stoichiometric and lean burn (λ=1.4) conditions.

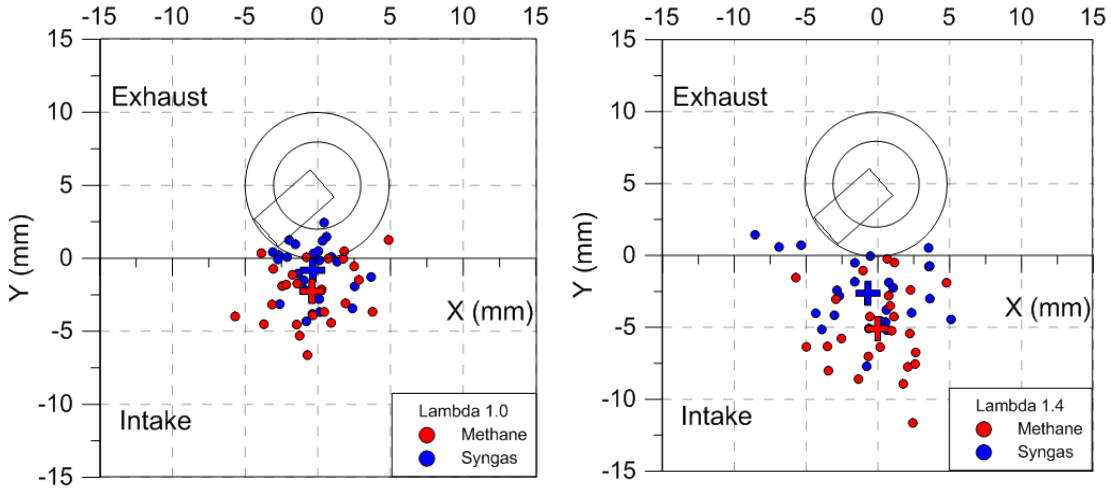

Figure 8. Luminous centroid measured for 25 engine cycles in correspondence of 5% MFB for both fuels in stoichiometric and lean burn (λ=1.4) conditions. Cross symbols referr to the average value.

4. CONCLUSIONS

The present paper resumes the results obtained by an experimental activity performed on a port fuel injection (PFI) spark ignition (SI) engine fueled with methane and an equivalent syngas representative of atmospheric gasification process. The target of the proposed research was to improve the knowledge on the combustion process when alternative

bio-derived fuels are used to replace fossil energy sources. For this reason, an optically accessible engine was used in order to integrate the results from thermodynamic analysis, based on in-cylinder pressure measurements, with cycle resolved flame visualization that featured high spatial and temporal resolution. The optical diagnostic, supported by a custom image processing methodology, permitted to characterize the flame front propagation in terms of size, velocity, shape and displacement. The experiments were carried out at low speed and wide open throttle, typical working point of SI engines for stationary applications. The effect of air dilution up to the point of methane flammability limit (λ=1.4) was investigated. Spark ignition timing was fixed in correspondence of MBT of methane in stoichiometric conditions. Syngas mixture demonstrated better performance and stability in lean burn condition than methane, even if the ignition setting was not optimized. Optical investigations demonstrated that the positive effect of syngas was due to a strong improvement in the flame front propagation during the early stages of combustion. As a consequence of higher flame speed, at 5% of MFB, the flame front of syngas fuel resulted less distorted and displaced from the combustion chamber center, compared to methane, and with a reduced cyclic spatial and temporal variability.

Even if further investigations are required to obtain deeper understanding of the effects of syngas composition on the combustion process and SI engine performance in a wide range of operative conditions, the current work represents a contribution to detailed database to validate numerical models and optimization codes.

5. ACKNOWLEDGEMENTS

This work was supported by CAPES and FAPESP.

6. REFERENCES

Agarwal, A.K., De, S., Pandey, A., Singh, A.P., 2017. “Combustion for Power Generation and Transportation”. *Springer Nature Singapore Ltd*. 2017 DOI 10.1007/978-981-10-3785-6.

Arroyo, J., Moreno, F., Muñoz, M., Monné, C., 2015. “Experimental study of ignition timing and supercharging effects on a gasoline engine fueled with synthetic gases extracted from biogas". *Energy Conversion and Management*, vol. 97: pp. 196-211.

Bika, A., Franklin, L., Kittelson, D., 2011. “Engine knock and combustion characteristics of a spark ignition engine operating with varying hydrogen and carbon monoxide proportions”. *International Journal of Hydrogen Energy*, vol. 36, pp. 5143-5152.

Catapano, F., Di Iorio, S., Sementa, P., and Vaglieco, B., 2013. “Characterization of CH_4 and CH_4/H_2 Mixtures Combustion in a Small Displacement Optical Engine”. *SAE Int. J. Fuels Lubr*. Vol. 6(1):pp.24-33, doi: 10.4271/2013-01-0852.

Di Iorio, S., Sementa, P, Vaglieco, B., 2015. “Analysis of combustion of methane and hydrogenemethane blends in small DI SI (direct injection spark ignition) engine using advanced diagnostics”. *Energy*, http://dx.doi.org/10.1016/j.energy.2015.09.012.

Di Iorio, S., Sementa, P, Vaglieco, B., 2014. “Experimental investigation on the combustion process in a spark ignition optically accessible engine fueled with methane/hydrogen blends”. *International journal of hydrogen energy*, vol. 18, pp. 9809-9823.

EPE (Empresa de Pesquisa Energetica), 2017, 1 Feb. 2017 <http://www.epe.gov.br>.

Hagos, F., Aziz, A., Sulaiman, S., 2014. “Effect of Air-fuel Ratio on the Combustion Characteristics of Syngas (H_2:CO) in Direct-injection Spark-ignition Engine”. *Energy Procedia*, vol. 61, pp. 2567-2571.

Heywood, J.B.,1998. “Internal Combustion Engine Fundamentals”. *McGraw-Hill*, New York, USA.

Irimescu, A., Marchitto, L., Merola, S.S., Tornatore, C., Valentino, G., 2014. “Evaluation of different methods for combined thermodynamic and optical analysis of combustion in spark ignition engines”. *Energy Conversion and Management*, Vol. 87, pp. 914-927, ISSN 0196-8904, http://dx.doi.org/10.1016/j.enconman.2014.07.037.

Martinez, S., Irimescu, A., Merola, S.S., Lacava, P., Curto-Riso, P., 2017. “Flame Front Propagation in an Optical GDI Engine under Stoichiometric and Lean Burn Conditions”. *Energies*, vol. 10, pp. 1337.

Martínez, J., Mahkamov, K., Andrade, R., Silva, L., 2012. “Syngas production in downdraft biomass gasifiers and its application using internal combustion engines”. *Renew Energy*, vol. 38, pp. 1–9.

Magalhaes, E.M., 2011 "Combustion study of mixtures resulting from a gasification process of forest biomass". Engineering Sciences. ISAEENSMA Ecole Nationale Superieure de Mecanique et d’Aerotechique - Poitiers, 2011.

Merola, S., Tornatore, C., Irimescu, A., 2016. “Cycle-resolved visualization of pre-ignition and abnormal combustion phenomena in a GDI engine”. *Energy Conversion and Management vol. 127 pp.380–391*.

Merola, S.S., Irimescu, A., Marchitto, L., Tornatore, C., Valentino, G., 2017.” Effect of injection timing on combustion and soot formation in a direct injection spark ignition engine fueled with butanol”. *Int. Journal of Engine Research*, 18 (5-6), pp. 490-504.

Parker, J. R., 2010. Algorithms for image processing and computer vision. John Wiley & Sons.

Shivapuji, A., Dasappa, S., 2015. "Influence of fuel hydrogen fraction on syngas fueled SI engine: Fuel thermo-physical property analysis and in-cylinder experimental investigations". *International Journal of Hydrogen Energy*, vol. 40, pp. 10308-10328.
U.S. Energy Information Administration, Electricity; 2017.

7. RESPONSIBILITY NOTICE

The authors Santiago Martinez, Simona Merola, Adrian Irimescu, Pedro Lacava, Pedro Curto and Maycon F Silva are the only responsible for the printed material included in this paper.